Technical Memorandum

To: Jeff Uhlmeyer

From: Lauren Gardner, Gonzalo Rada, and Kevin Senn

cc: Mustafa Mohamedali

Date: December 11, 2020

Re. Forensic Desktop Study Report: Minnesota LTPP Test Section 27_6251

The Long-Term Pavement Performance GPS-1 Asphalt Concrete (AC) Pavement on Granular Base test section 27_6251[1] was nominated for a desktop study under TPF-5(332) "LTPP Forensic Evaluations." The test section was incorporated into the LTPP program in 1987 and moved to the GPS-6S AC Overlay of Milled AC Pavement Using Conventional or Modified Asphalt in 1998 after receiving a 1.6-inch mill and a 3.4-inch AC overlay. This site was also included in the LTPP Seasonal Monitoring Program (SMP) between 1993 and 2003. As part of the SMP, the section was instrumented with an on-site weather station, along with subsurface temperature, moisture, frost detection, and water table depth sensors. The collection of FWD measurements and the downloading of the climatic information were performed monthly, and data collection of profile measurements were conducted quarterly. As a test section with particularly rich data, an investigation and comparison of the performance of the pavement over time was conducted. This desktop study examines 1) the relationship between pavement deflection, pavement temperature, and subgrade moisture content, 2) the cause(s) for the reduction in the reported fatigue cracking area between 2015 and 2016, 3) whether any of the non-wheel path longitudinal cracking or transverse cracking observed prior to the mill and overlay is reflected following the mill and overlay, and 4) the reason(s) for the extremely low IRI on the pavement section following the overlay despite the presence of cracking throughout time.

SITE DESCRIPTIONS

LTPP test section 27_6251 was located on U.S. Route 2, westbound, in Beltrami County, Minnesota. U.S. Route 2 is a rural principal arterial with two lanes in the direction of traffic. The test section was classified as being in a Wet, Freeze climate zone. While at the time of its nomination the site was considered active, based on information in the LTPP database, the test section has since been found to be milled and overlaid and therefore has been placed Out of Study (OOS). The coordinates (in degrees) of the site were 47.46124, -94.912. Photograph 1 shows the section at Station 0+00 looking westbound in 2017, while Map 1 shows the geographical location of the test section.

[1] First two digits in test section number represent the State Code [27 =Minnesota]. The final four digits are unique within each State/Province and were assigned at the time the test section was accepted into the LTPP program.

Wood Environment & Infrastructure Solutions, Inc.
12000 Indian Creek Ct, Suite F
Beltsville, MD 20705
+1 301-210-5105
www.woodplc.com

Photograph 1. LTPP Section 27_6251 at Station 0+00 looking westbound in 2017.

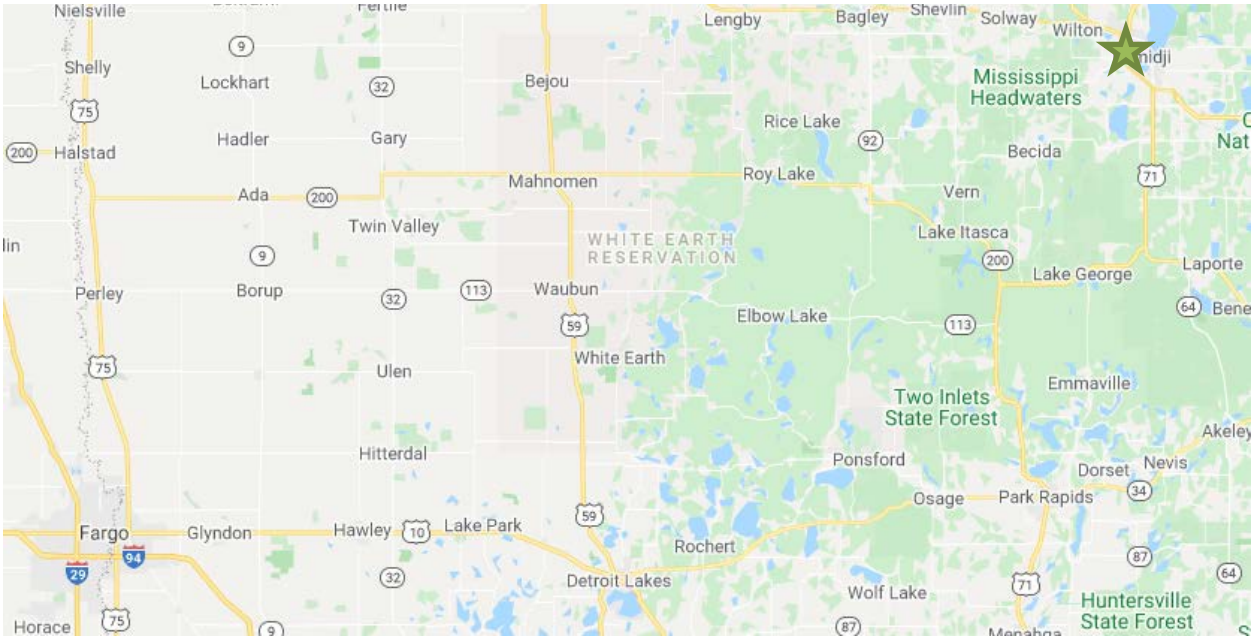

Map 1. Geographical location of LTPP Section 27_6251.

BASELINE PAVEMENT HISTORY

This section of the memorandum presents historical data on the pavement structure and its structural capacity, climate, traffic, and pavement distresses.

Pavement Structure and Construction History

The test section was constructed in September 1981 and was accepted into the LTPP Program as part of the GPS-1 experiment in January 1987. The pavement structure at the time of its incorporation into the LTPP program consisted of 7.4 inches of dense-graded asphalt concrete (AC) and 10.2 inches of unbound (granular) base over a coarse-grained subgrade layer. This pavement structure is summarized in Table 1 and corresponds to CONSTRUCTION_NO = 1 (CN = 1) in the LTPP database. The next construction event occurred in June 1998, when the test section received 1.6-inch mill and a 3.4-inch AC overlay. Subsequently, the test section was moved to the GPS-6S AC Overlay of Milled AC Pavement Using Conventional or Modified Asphalt study. Table 2 summarizes the pavement structure following the mill and overlay, which corresponds to CONSTRUCTION_NO = 2 (CN = 2). Additional construction events that occurred on the site included crack sealing in both June 2001 and June 2015 (CN=3 and CN=4) and skin patching in June 2016 (CN=5). However, these construction events did not change the overall structure of the pavement section. The test section was found to be milled and overlaid sometime after the last survey date in 2017 (the specific year of the event is still being determined), and therefore, the site has been placed Out of Study (OOS).

Table 1. Pavement structure for 27_6251 (CN=1)

Layer Number	Layer Type	Thickness (in.)	Material Code Description
1	Subgrade (untreated)		Coarse-Grained Soils: Poorly Graded Sand with Silt
2	Unbound (granular) subbase	10.2	Gravel (Uncrushed)
3	Asphalt concrete layer	7.4	Hot Mixed, Hot Laid AC, Dense Graded

Table 2. Pavement structure for 24_1634 (CN=2) to present

Layer Number	Layer Type	Thickness (in.)	Material Code Description
1	Subgrade (untreated)		Coarse-Grained Soils: Poorly Graded Sand with Silt
2	Unbound (granular) subbase	10.2	Gravel (Uncrushed)
3	Asphalt concrete layer	5.8	Hot Mixed, Hot Laid AC, Dense Graded
4	Asphalt concrete layer	3.4	Recycled AC, Hot Laid, Central Plant Mix

Pavement Structural Properties

Figure 1 and Figure 2 show the average Falling Weight Deflectometer (FWD) deflections under the nominal 9,000-pound load plate during the entire period the test section was in study (Figure 1) and during the SMP analysis period (Figure 2). The deflection of the sensor located in the center of the load plate is a general indication of the total "strength" or response of all layers in the pavement structure to a

vertically applied load. Similarly, Figure 3 shows the average deflection at the sensor farthest from the load plate (60" from the center load plate) during the SMP analysis period.

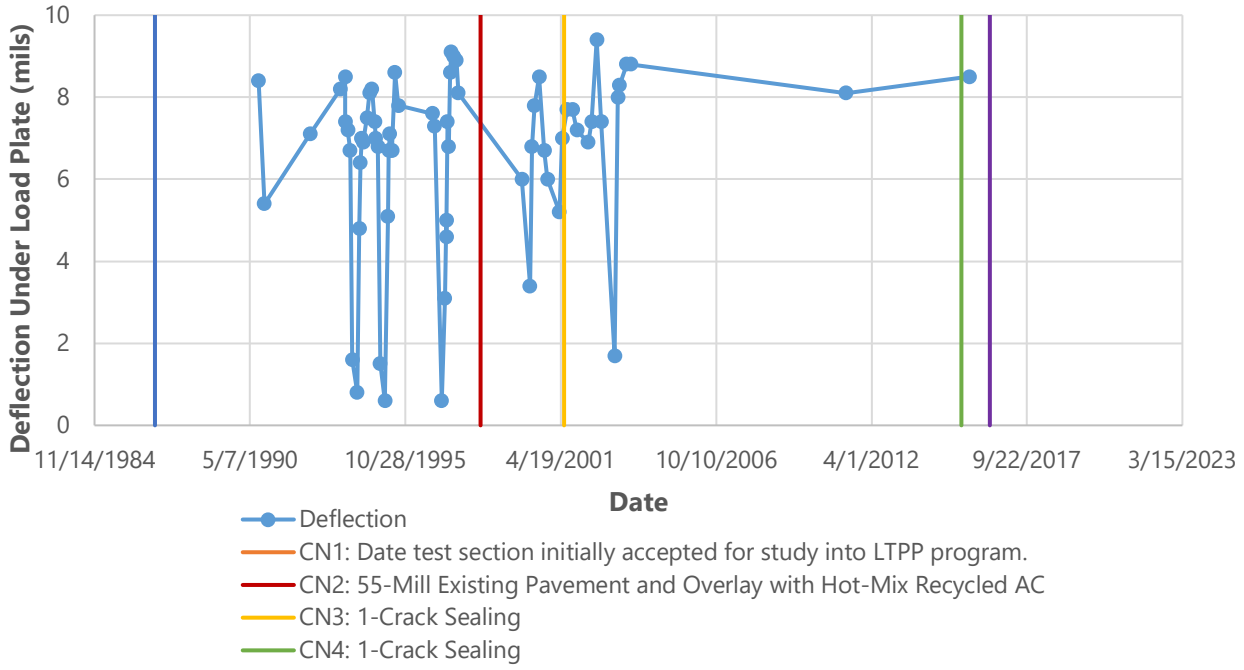

Figure 1. FWD deflections under the load plate over time.

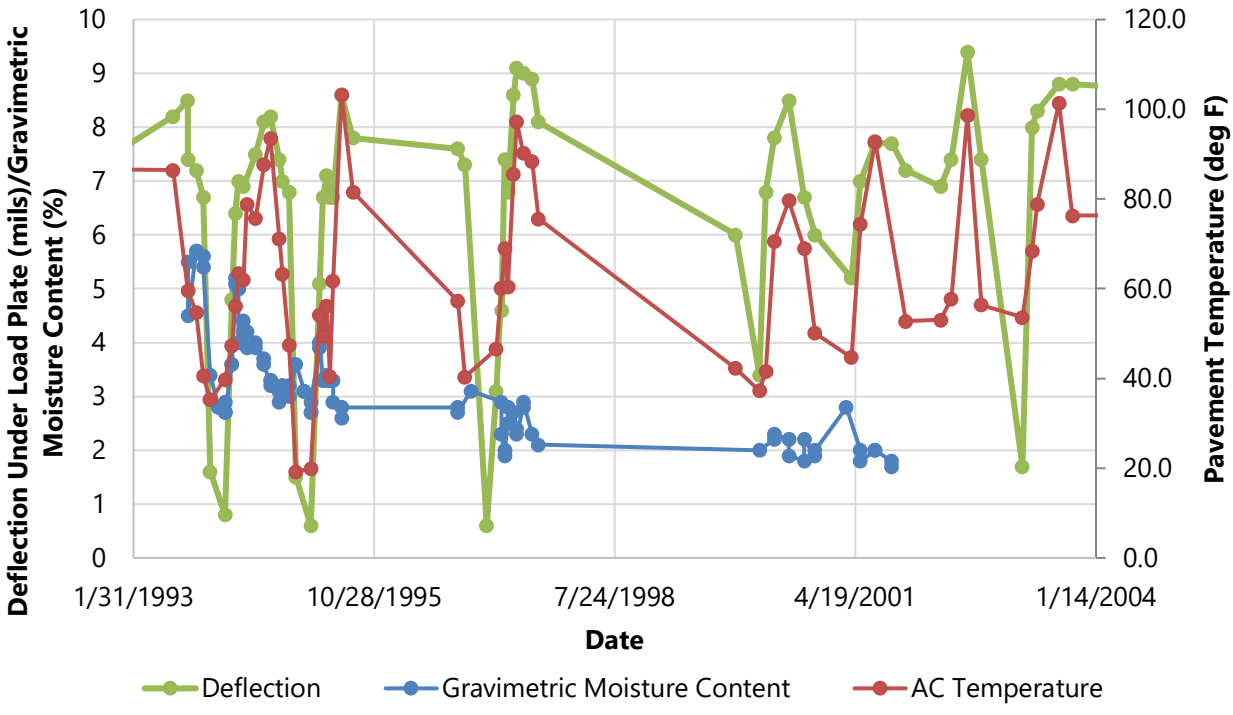

Figure 2. Comparison of a) FWD deflections under the load plate (Sensor 1), b) the average temperature of the pavement taken at a depth of 1-inch below the surface, and c) the gravimetric moisture content at a depth of 24 inches below the surface of the pavement (TDR 3).

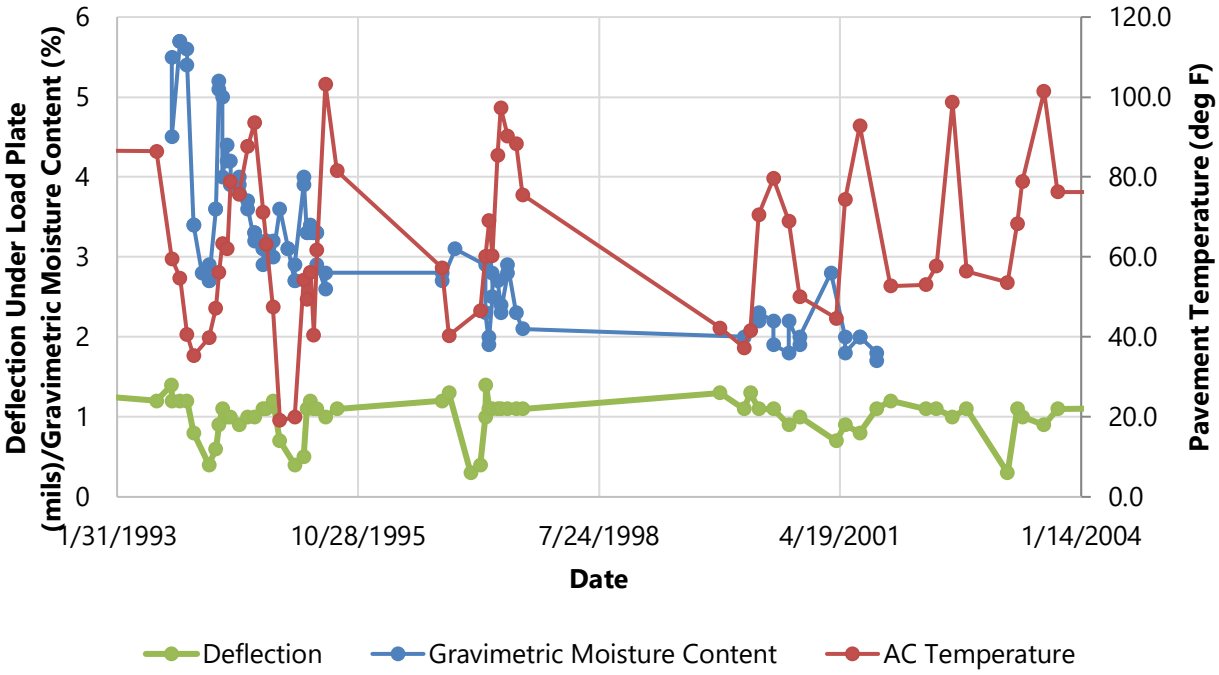

Figure 3. Comparison of a) FWD deflections the sensor farthest from the load plate (60"), b) the average temperature of the pavement taken at a depth of 1-inch below the surface, and c) the gravimetric moisture content at a depth of 24 inches below the surface of the pavement (TDR 3).

Because of how the FWD (or other) load is distributed on an AC pavement, deflections at the farthest sensor are due almost in their entirety to the subgrade response (i.e., little to no influence from AC and base layers). As shown in Figure 2 and Figure 3, the deflections observed can be influenced by pavement temperature at the time of testing and moisture conditions. The gravimetric moisture content shown in both figures was calculated from Time Domain Reflectometry (TDR) sensor data collected at a depth of 24 inches below the surface of the pavement, i.e., within the subgrade. The pavement temperature depicted in the figures represents the average pavement temperature at the time of testing 1-inch below the surface (measured during FWD testing), i.e., within the AC layer.

As depicted in Figure 2, the change in deflection under the load plate over time appears to be directly related to the change in pavement temperature over time. For the most part, increases and decreases in deflections correspond to increases and decreases in the pavement temperature. The relationship between the average deflection and moisture content of the test section is less clear. It is generally expected that as the moisture content increases, deflections will also increase, but this does not appear to be the case.

In Figure 3, on the other hand, the change in deflection measured at the farthest sensor from the load plate appears to have little relationship with both the change in moisture content and the change in temperature over time. It is generally expected that as the moisture content increases, deflections will also increase, but this does not appear to be the case.

The layer moduli backcalculated from the deflection data were also assessed for the test section. The pavement structure was modeled as 7.4 inches of AC and 10.2 inches of granular base over subgrade (divided into two layers). Following CN=2 in 1998, the pavement structure for the test section was modeled as 9 inches of AC and 10.2 inches of granular base over subgrade (divided into two layers). It is important to note that the representative AC thickness used for the backcalculations after CN=2 was 0.2-inch less than the reported thickness of the section in the TST_L05B table. While the difference in the

reported thickness and the thickness used for backcalculations is small, additional information on the reason(s) for the deviation should be pursued. The backcalculated moduli for each layer between August 1990 and May 2011 (59 dates in total) are shown in Figure 4 to Figure 7. The collection of FWD data in 2015 was performed after the completion of LTPP contract to backcalculate moduli data, and therefore backcalculated moduli were not included in the LTPP database.

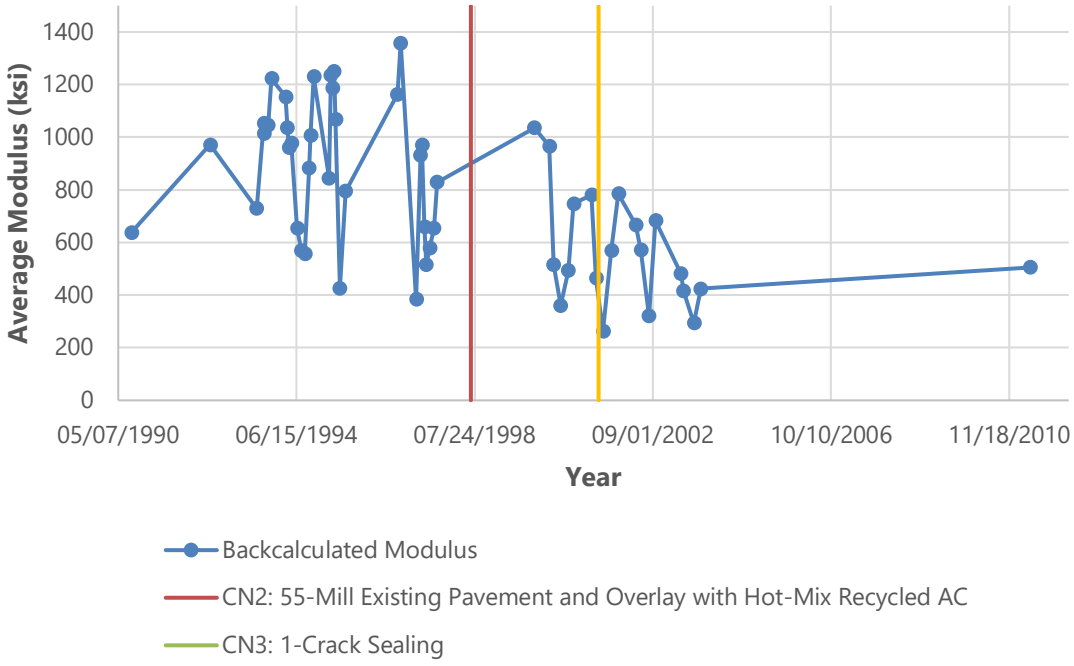

Figure 4. Average backcalculated modulus for AC (Layer 1).

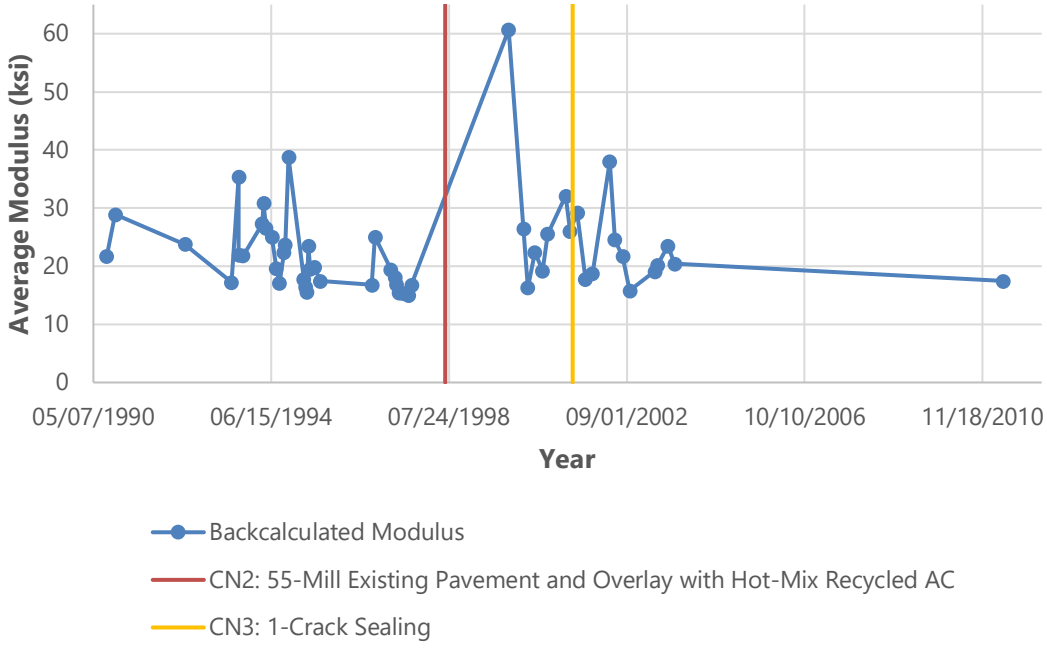

Figure 5. Average backcalculated modulus for granular base (Layer 2).

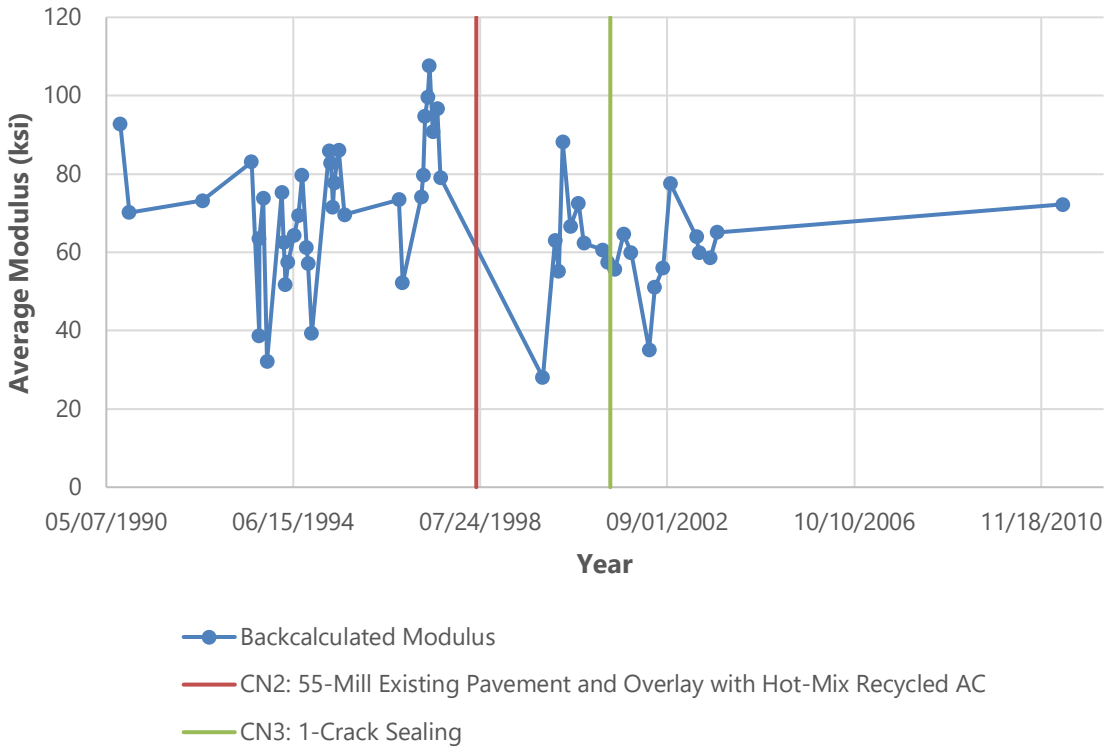

Figure 6. Average backcalculated modulus for top 24 inches of subgrade (Layer 3).

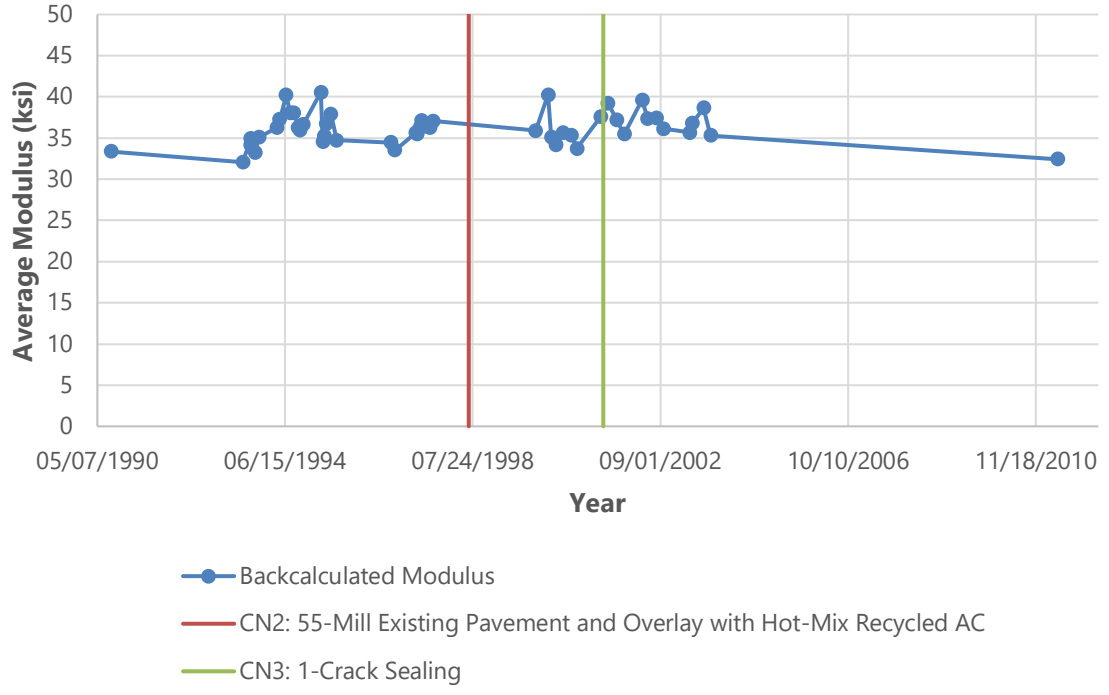

Figure 7. Average backcalculated modulus for subgrade (Layer 4).

For the most part, the range of moduli values calculated for each layer appear to be reasonable. However, for each layer, statistical outliers were removed from the dataset. This included data from:

- November 1990 (2,269 ksi), December 1994 (7,902 ksi), April 1997 (2,101 ksi), and March 2000 (1,941 ksi) for the AC layer,
- November 1993 (62 ksi), March 1994 (46 ksi), December 1994 (195 ksi), April 1997 (69 ksi), March 2000 (174 ksi) for the base layer,
- December 1994 (148 ksi), March 1995 (126 ksi), and March 1997 (134 ksi) for the top 24 inches of subgrade, and
- November 1990 (30 ksi), June 1992 (30 ksi), March 1994 (66 ksi and 43 ksi), December 1994 (60 ksi), March 1995 (69 ksi), March 1997 (93 ksi), April 1997 (43 ksi), and April 2001 (47 ksi) for the bottom subgrade layer.

With the outliers removed, the range of modulus values for the AC, base, top 24 inches of the subgrade, and the bottom subgrade layers was 263 ksi –1,359 ksi, 15 ksi –61 ksi, 28 ksi –108 ksi, and 32 ksi –41 ksi, respectively. For all four layers, the moduli appear to peak during winter months when the ground is likely to be frozen, and the moduli decrease during the spring and summer months when the layers are undergoing a thaw period (during spring) and become less stiff than when frozen.

The reasonableness of the backcalculated layer moduli was compared to moduli derived from laboratory resilient modulus testing. Table 3 summarizes the laboratory test results for the AC, subbase, and subgrade layers. For the AC layer, moduli values are shown for three test temperatures – 41, 77 and 104°F, respectively. As shown in Figure 8, the AC modulus versus temperature relationship for the field- and lab-derived resilient moduli appears to be reasonable; while there is some scatter due to the variation in backcalculated moduli results, there appears to be a clear trend between temperature and the AC layer modulus. For the unbound granular base and subgrade layers (which correspond to Layer 2 and Layers 3 and 4 of the backcalculated moduli, respectively), various statistical analyses were conducted for the range of stress states (confining and deviatoric stresses) to which the laboratory samples were subjected. While the range of values in the base are similar to the backcalculated values reported for Layer 2, the laboratory values for the subgrade were slightly lower than the backcalculated moduli reported for Layers 3 and 4. However, overall, the values appeared reasonable given the pavement structure.

Table 3. Laboratory Resilient Modulus Test Results

Layer	Temperature (°F)	Number of Samples/test results	Range of moduli values (ksi)	Range of Confining Stress (psi)	Range of Maximum Nominal Axial Stress (psi)
AC	41	1 sample (2 tests, original AC layer)	2,178-2,190	N/A	N/A
	77	1 sample (2 tests, original AC layer)	567-663	N/A	N/A
	104	1 sample (2 tests, original AC layer)	129-236	N/A	N/A
Base	N/A	1 sample (15 test results each)	10.7 to 41 (Average of 24.1)	3 to 20	3 to 40
Subgrade	N/A	2 samples (15 test results each)	4.9 to 13.1 (Average of 9.1)	2 to 6	2 to 10

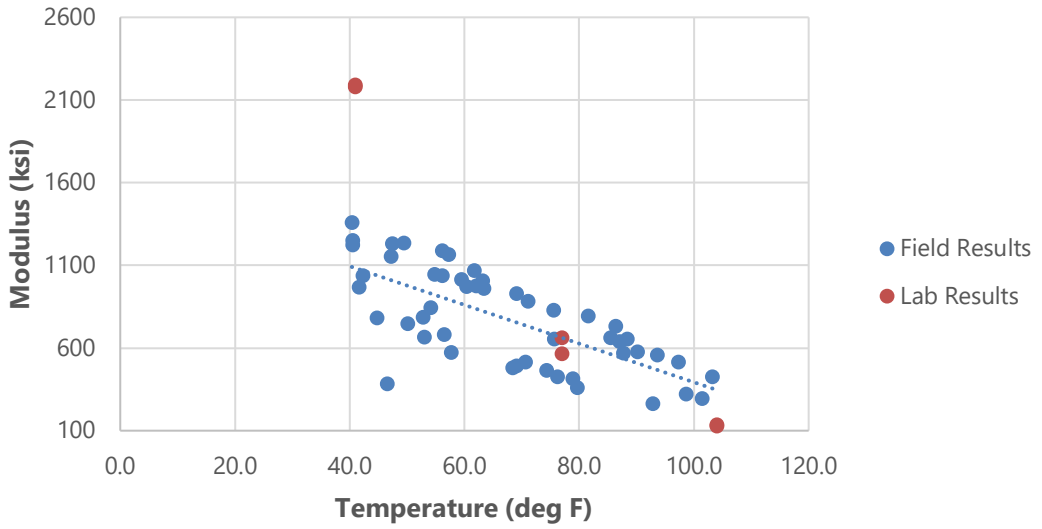

Figure 8. Field- and lab-derived AC resilient modulus values.

Deflection Regression Analyses

A multiple linear regression analysis like the one applied for the test sections 30_8129 (Montana) and 24_1634 (Maryland) was performed for the Minnesota test section 27_6251. The objective of this analysis was to statistically relate variations in deflection to changes in the pavement temperature, subgrade moisture content, and the measurement position. The position variable was defined as a categorical variable; its value was either 0 for the measurements obtained under the center of the load plate or 1 for the measurements captured at the sensor farthest from the load plate. The deflection data at both positions of 0 and 1 were collected from 1990 to 2015. Table 4 gives an overview of the data for the pavement temperature and subgrade moisture variables gathered during the deflection data collection period, including their mean, minimum, and maximum values. It was noticed that the deflection data collected after November 2001 had missing in-situ subgrade moisture values (reported in SMP_TDR_AUTO_MOISTURE). The LTPP SMP_TDR_AUTO_MOISTURE_TLE table was used to fill some of the missing values for years between 2001 to 2003.

Table 4. Summary Statistics for pavement temperature and subgrade moisture content data.

Summary Statistic	Pavement Temperature	Subgrade Moisture
Mean	63.80 °F	3.13 %
Minimum	19.14 °F	1.75 %
Maximum	103.24 °F	5.70 %

In the regression analysis, the mean was subtracted from the observed values for the temperature and moisture variables. The updated means of the temperature values and moisture values were equal to 64.42 °F and 3.43%, respectively. Table 5 shows the outputs of the regression analysis. As shown, the regression coefficients for pavement temperature and moisture content are positive, which means that if either of these factors increases, the average pavement deflections will also increase. In addition, based on the computed p-values, it is apparent the variation in the average deflection is highly correlated with changes in temperature, moisture content, and position.

Table 5. Regression analysis results.

Factor	Regression Coefficient	P-value
Intercept	6.7753	< 2e-16
Temperature	0.0867	< 2e-16
Moisture	0.4452	6.95e-05
Position	-5.7641	< 2e-16
Temperature * Position	-0.0838	3.64e-14
Moisture * Position	-0.4121	0.00757

The effect of temperature–position and moisture–position interactions on the deflections were also considered. The interaction between two factors is said to occur when the magnitude of the effect of one factor on the dependent variable changes as the level of the other variable changes. Table 5 shows that these interaction effects are statistically significant and that they have a negative effect on the average pavement deflection. The impacts of these interactions are shown graphically in Figure 9 and Figure 10. The effects of AC temperature and moisture content on deflection are significant for position 0, while they are less significant in position 1.

The regression analysis yielded the following model to predict pavement deflection (mils) based on pavement temperature (°F), subgrade moisture content (%), and measurement position (0 or 1):

$$Deflection = 6.78 + 0.087 * (Temperature - 64.42) + 0.45 * (Moisture - 3.43) - 5.76 * Position - 0.084 * (Temperature - 64.42) * Position - 0.41 * (Moisture - 3.43) * Position$$

At position 0 (under center of load plate), the above equation reduces to:

$$Deflection = 6.78 + 0.087 * (Temperature - 64.42) + 0.45 * (Moisture - 3.43)$$

While at position 1 (farthest sensor from center of load plate), the equation reduces to:

$$Deflection = 1.02 + 0.003 * (Temperature - 64.42) + 0.04 * (Moisture - 3.43)$$

The scatter plot of the predicted deflection values from the model versus the actual measured deflection values is shown in Figure 11. This plot shows a good correlation between measured and predicted deflection values with a coefficient of determination (R^2) of 0.92. The R^2 shows that 92% variability of deflection data can be explained by the variables in the model.

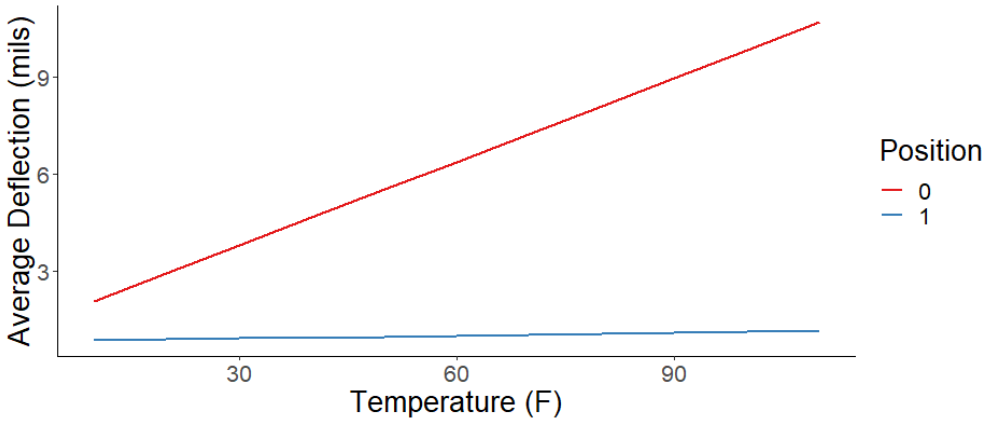

Figure 9. Interaction plot of temperature and position.

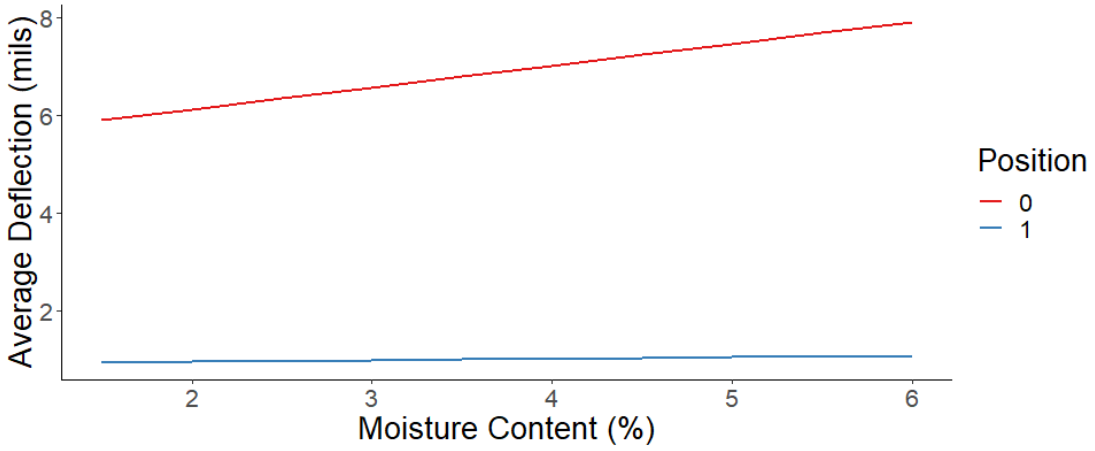

Figure 10. Interaction plot of temperature and position.

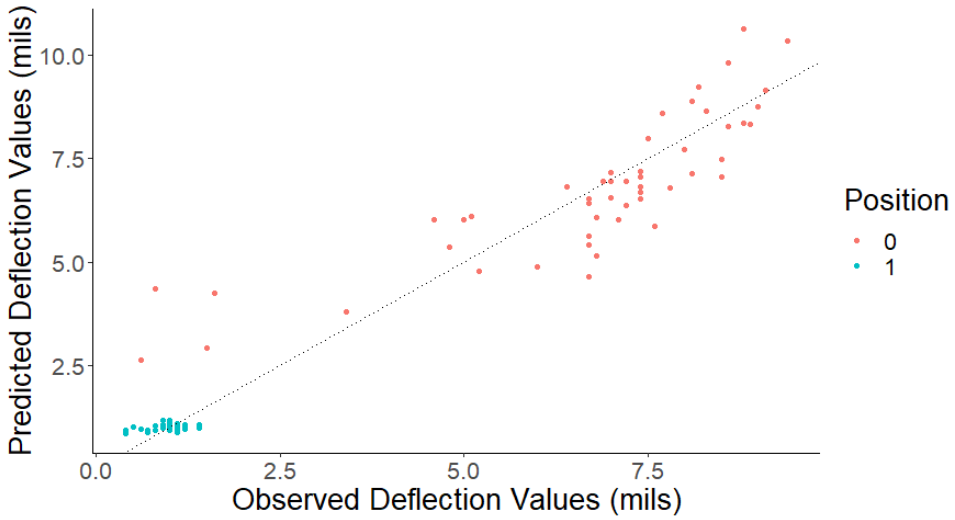

Figure 11. Predicted versus observed values of pavement deflection.

Climate History

The time history for average annual precipitation (from Modern-Era Retrospective analysis for Research and Applications or MERRA) since 1981 is shown in Figure 12. Prior to the mill and overlay event in 1998, the average yearly precipitation was approximately 29.5 inches. Following the mill and overlay event, the average yearly precipitation was slightly higher; approximately 31.8 inches.

Figure 13 shows the time history of the average annual freezing index (from MERRA) for the test site. The freezing index is the summation of the difference between freezing temperature and the average air temperature when it is less than freezing over a year's time. This index is an indicator of the harshness of the winter season relative to issues such as ground frost and low temperature cracking in pavements. As depicted in Figure 13, the freezing index values ranged from 1,649 deg F deg days (2012) to 4,037 deg F deg days (1996). During the first performance period, prior to the mill and overlay event (1981-1997), the average annual freezing index was 2,875 deg F deg days. Following the mill and overlay event, between 1998 and 2019, the average annual freezing index decreased to 2,459 deg F deg days. All freezing indices reported during the analysis period are well above the 150 deg F deg days used to classify a freeze region.

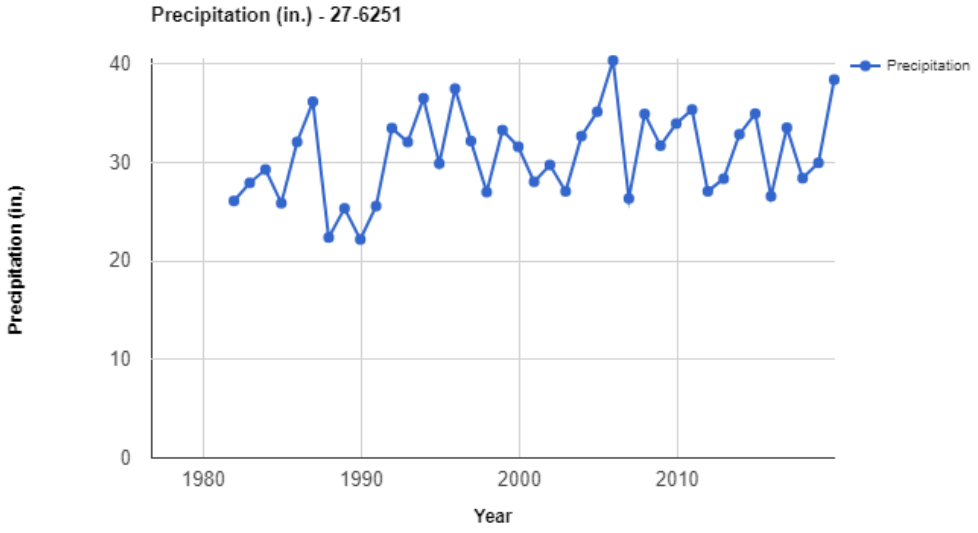

Figure 12. Average yearly precipitation over time.

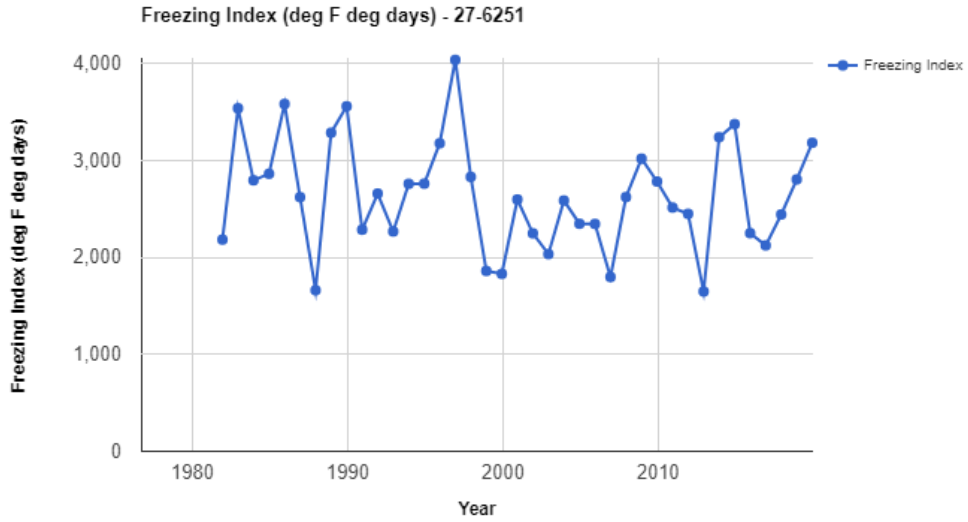

Figure 13. Average annual freezing index over time.

Truck Volume History

Figure 14 shows the annual average daily truck traffic (AADTT) data in the LTPP test lane by year. The annual truck traffic increased from 222 in 1981 to 769 in 2017, or approximately 15 additional trucks per day per year. The average number of ESALs reported on the section also increased over time as depicted in Figure 15. The number of ESALS increased from 11,029 in 1981 to 151,570 in 2017. A combination of historical AADTT values (1981-1989), state provided AADTT values (1990 and 1996-1998), monitored values (1991-1995), and values calculated using a compound growth function (1999-2017) were used to report traffic along these test sections. Additionally, for the ESAL data reported in years when a major construction event occurred (such as the mill and overlay in 1998 and crack sealing in 2001 and 2015), the average annual ESALs was reported twice—once using data collected prior to the construction event and a second time after the construction event. For example, in 1998, when the mill and overlay event occurred

on the test section, the average annual ESALs for the section was calculated using State provided AADTT data collected before the June mill and overlay (data collected between January and June of 1998) and separately using data collected after the mill and overlay event (data collected between July and December of 1998). In the figure below, the ESALs reported show both sets of data, color-coded by the CN event they describe.

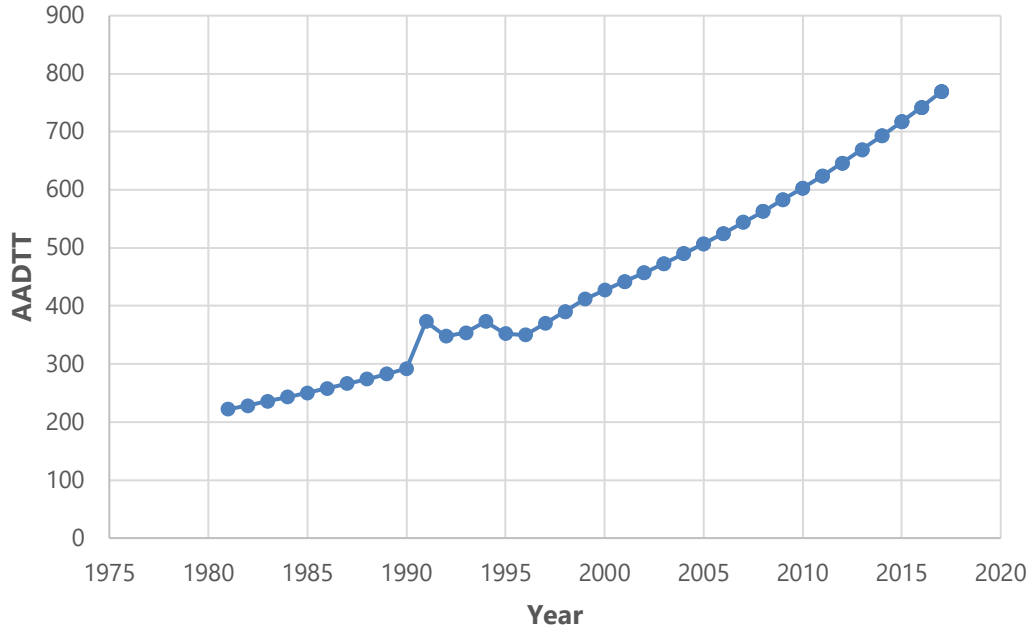

Figure 14. Average annual daily truck traffic (AADTT) history.

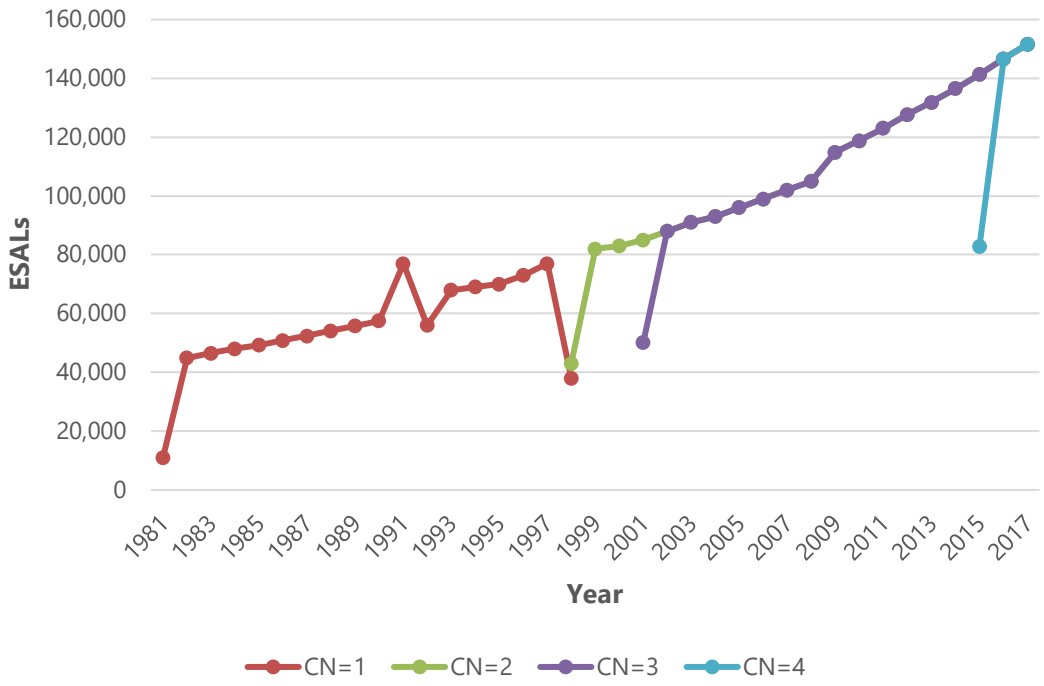

Figure 15. Estimated annual ESAL for vehicle classes 4-13 over time by CN.

Pavement Distress History

The following summarizes the distresses observed on the test section, which was last monitored in 2017. This is also the final monitoring that took place on the test section as it is now OOS. Fatigue/alligator cracking, longitudinal cracking, transverse cracking, IRI, and rutting were assessed.

Fatigue/Alligator Cracking

Figure 16 shows the total area in which fatigue/alligator cracking was observed for the section between 1992 and 2016. While the graph obtained from InfoPave™ is labelled fatigue cracking, which implies a mechanism, the distress values reported includes both fatigue cracking (inside the wheel path) and alligator cracking (outside the wheelpath).

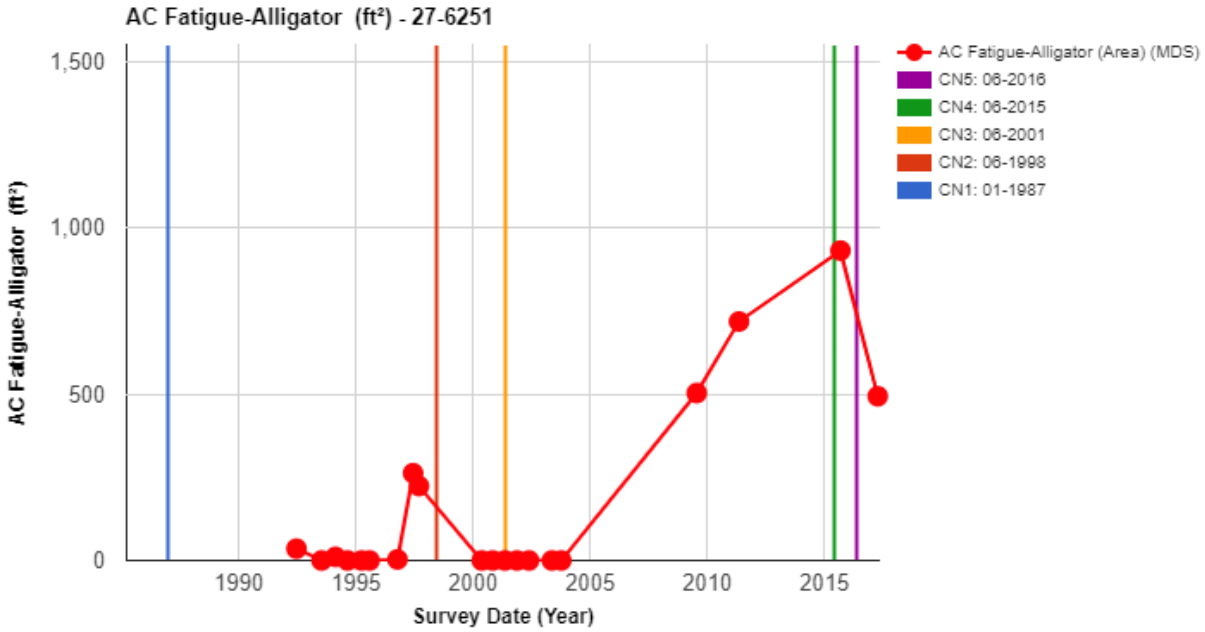

Figure 16. Time history of the length of fatigue cracking.

Fatigue/alligator cracking was first reported during the manual distress survey in 1992, when 36 ft^2 was observed. The fatigue/alligator cracking observed decreased between 1992 and 1993, before increasing again in 1997 when 224 ft^2 was reported. Following the mill and overlay in June 1998, no fatigue/alligator cracking was observed until the 2009 distress survey, 11 years after CN=2, when 504 ft^2 of fatigue/alligator cracking was reported. Once observed, the cracking propagated at a rate of 71 ft^2/year between 2009 and 2015, reaching 932 ft^2 in 2015. However, in April 2017, following the skin patching event in June 2016, the fatigue/alligator cracking observed decreased to 494 ft^2. The drop in fatigue/alligator cracking in 2016 is likely due to a combination of the differences in rater opinions between the 2015 and 2017 surveys and the effects of the skin patching that occurred in 2016 (CN=5). As shown in Figure 17, while fatigue/alligator cracking is mostly reported in the same locations in 2015 and 2017, the rater in 2015 reported larger areas of low severity fatigue/alligator cracking (3.3-foot width in the wheel path compared to a 2-foot width reported in 2017) while the 2017 rater reported smaller areas of medium and high severity fatigue/alligator cracking. This figure also shows, under the comments section for the 2017 survey, that the rater found inconsistencies with the 2015 survey's drawings and quantities. In addition to the differences in the width of fatigue cracking reported between the two years, additional fatigue/alligator cracking (~13.5 ft^2) was reported between stations 3+00 and 3+50 in 2015, but not in 2017. This is likely due to the difficulty in rating low severity fatigue/alligator cracking. Finally, the patching that took place in 2016, reported as 7L in Figure 17, also seems to have played a role in the overall cracking reported in 2017.

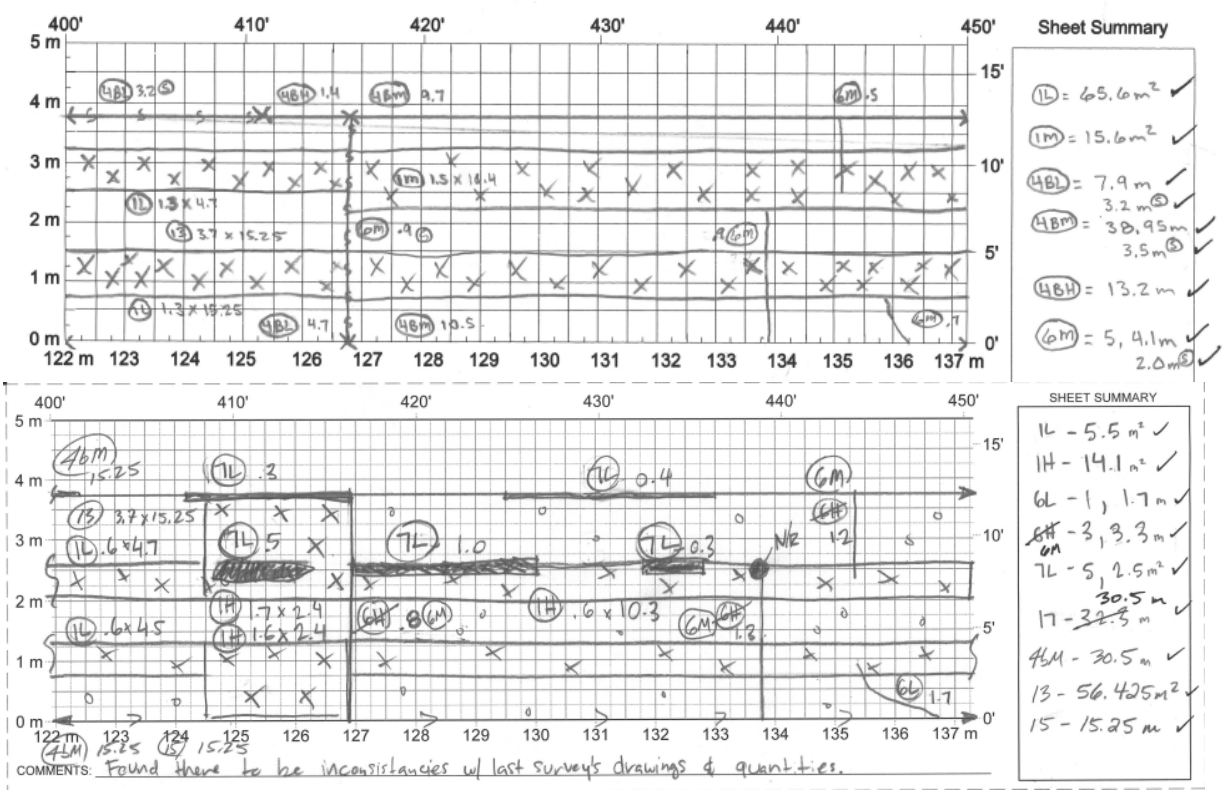

Figure 17. Fatigue cracking on the section in 2015 (top) and 2017 (bottom).

The increase in fatigue/alligator cracking following CN=3 seems to be related to pavement aging and overall structural degradation. The original structure was constructed in 1981 and therefore, may have been experiencing increased cracking due to long-term environmental exposure (high levels of precipitation and freeze-thaw) and traffic loadings. This hypothesis is further supported by the high amounts of material degradation (raveling and pumping) reported throughout the section during the last three pavement distress surveys. Another factor that could have contributed to the increase in fatigue/ alligator cracking after CN=3 is the increased precipitation observed during the performance period following the mill and overlay in 1998. As noted earlier, prior to the mill and overlay event in 1998, the average yearly precipitation was approximately 29.5 inches. Following the mill and overlay event, the average yearly precipitation was slightly higher; approximately 31.8 inches. As water infiltrates the pavement, unbound granular layers tend to weaken (especially when reaching saturation conditions), which can contribute to the observed fatigue/alligator cracking.

Longitudinal Cracking

Non-wheel path (NWP) longitudinal cracking, depicted in Figure 18, was reported during the first manual distress survey in 1992, when 804 ft of cracking was observed. The NWP longitudinal cracking observed slightly increased between 1992 and 1997 at a rate of 3.8 feet/year. After the mill and overlay in June 1998, the NWP longitudinal cracking observed during the next distress survey in May 2000 decreased to 302 feet. However, the NWP longitudinal cracking again increased at a rate of 41 feet/year between 2000 and 2017, with a reported 1,000 feet of cracking by April 2017. Upon further inspection of the location and severity of the non-wheel path longitudinal cracking on the test section, it was found that the cracking reported in the LTPP AC distress summary table (MON_DIS_AC_REV) did not align with the distresses reported in manual distress surveys prior to 1998 mill and overlay. The values reported in InfoPave™ were

approximately double that of the distresses reported in the manual distress surveys. The discrepancy between the LTPP database and the manual distress surveys is recommended for further investigation.

The NWP longitudinal cracking reported prior to the mill and overlay was predominantly located on the edge of the lane and between the wheel paths. After the overlay, the cracking was predominantly observed on the edge and centerline of the lane. Given the cracking location, it is hypothesized that the propagation of the NWP longitudinal cracking is construction related (rather than reflection cracking) as it appears the cracking may be located along construction joints.

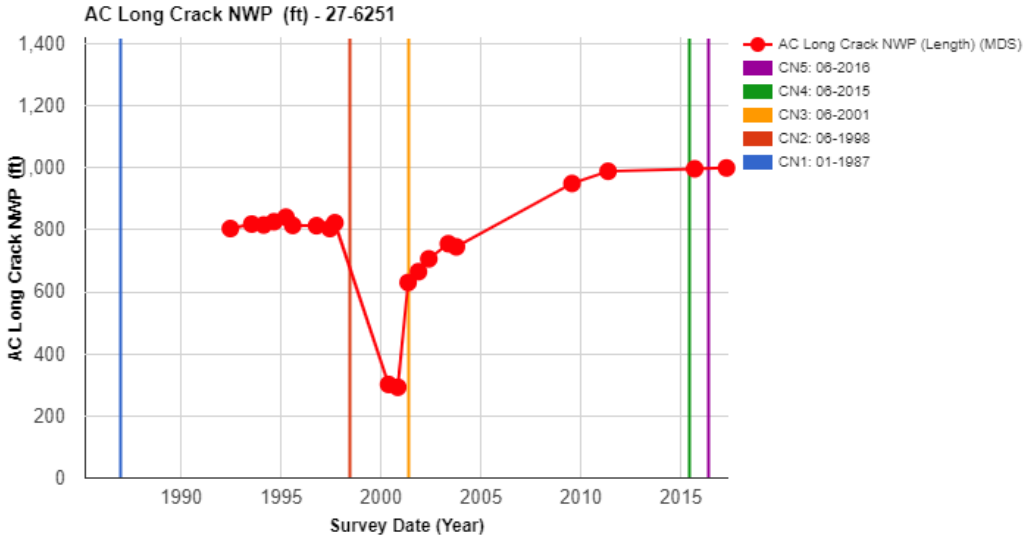

Figure 18. Time history of the length of NWP longitudinal cracks.

Wheel path (WP) longitudinal cracking, depicted in Figure 19, was reported during the first manual distress survey in 1992, when 42 ft of cracking was observed. The WP longitudinal cracking observed increased between 1992 and 1997 at a rate of 50 feet/year, reaching 290 feet in 1997. After the mill and overlay in June 1998, no WP longitudinal cracking was observed. This is likely because wheel path cracking after the mill and overlay was rated as fatigue/alligator cracking.

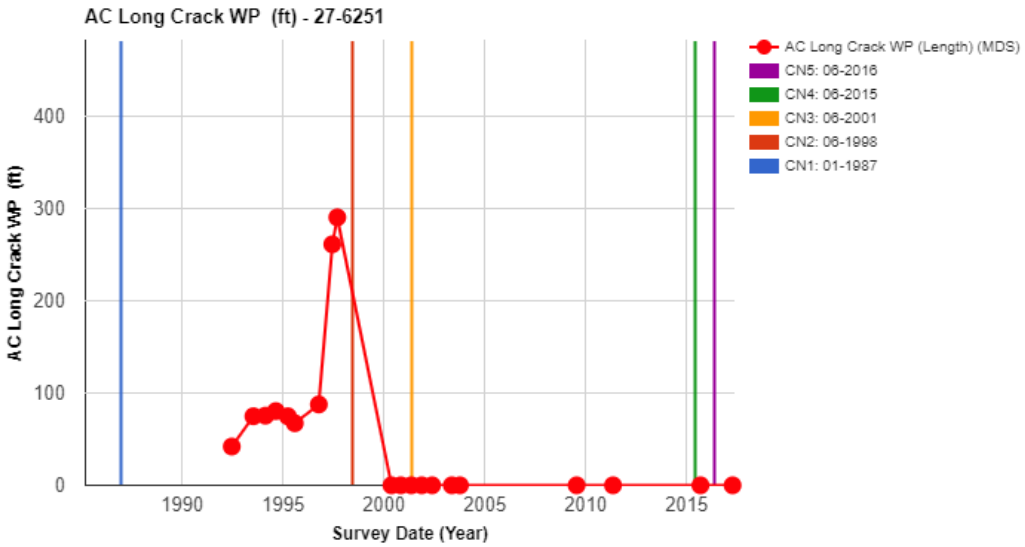

Figure 19. Time history of the length of WP longitudinal cracks.

Transverse Cracking

Data on transverse cracking was collected between 1992 and 2017 as shown in Figure 20 and Figure 21. Transverse cracking was first reported during the manual distress survey in 1992, when 344 ft of cracking (37 cracks) was observed. The transverse cracking fluctuated between 1992 and 1997, reaching 394 ft (45 cracks) in 1997. Following the mill and overlay in 1998, the reported transverse cracking dropped to 137 feet (13 cracks) during the next manual distress survey in May 2000. Between 2000 and 2017, the reported cracking increased at a rate of 8.4 feet/year, reaching 280 feet (35 cracks) by 2017.

Both prior to and following the mill and overlay event in 1998, transverse cracking was located in similar locations, indicating transverse cracking observed prior to the overlay event was reflected to the overlay surface. It is hypothesized that the propagation of the transverse cracking is primarily related to the freeze-thaw periods (evidenced by the high freezing indices) of the pavement section over time. This explanation would also justify the greater length of transverse cracking prior to the mill and overlay event as the average annual freezing index, and therefore, the assumed harshness of the freeze-thaw, during this performance period was slightly higher than after the mill and overlay. Another explanation is that the relative stiffness of the original AC layer was greater than relative stiffness of the overlay layer (as evidenced by the backcalculated moduli). With the original AC layer being stiffer, the freeze-thaw period would cause more transverse cracking prior to the mill and overlay.

IRI

The average IRI measurements for the section over time are shown in Figure 22. During the first performance period of the test section, from its incorporation into the LTPP program to the mill and overlay event in 1998, the IRI on the test section increased over time. The IRI on the section, prior to the mill and overlay event in 1998, was 182 in/mi, which means the performance of the pavement was classified as "Poor" based on FHWA performance definitions. After CN=2, the IRI of the test section dropped to 42 in/mile in 1999 before increasing again at a modest but steady rate of 1.5 in/mi/year between December 1999 and April 2017. The average IRI during this performance period is classified as "Good" based on FHWA performance definitions.

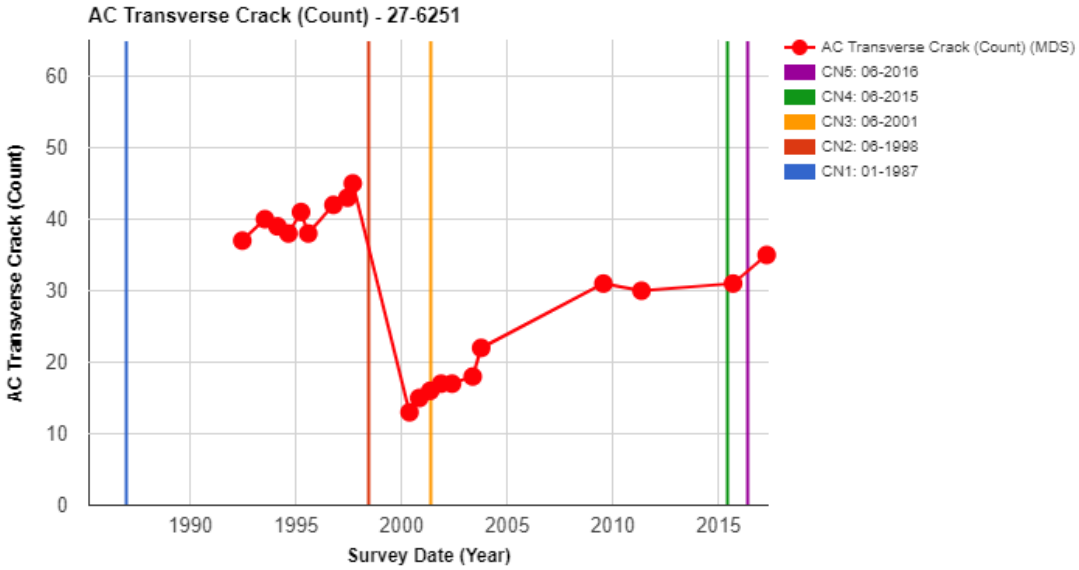

Figure 20. Time history of the number of transverse cracks.

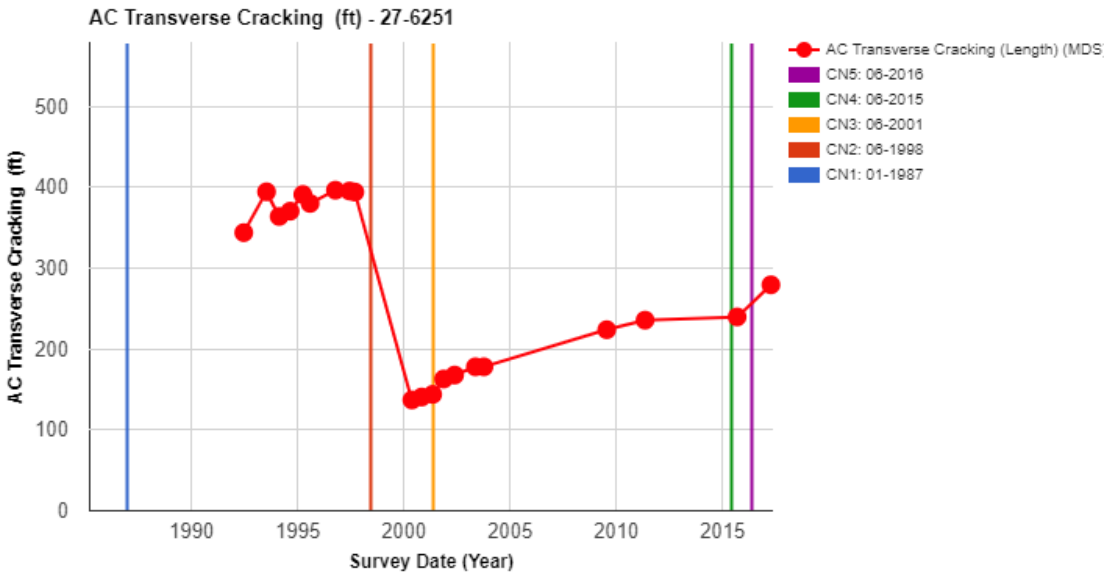

Figure 21. Time history of the length of transverse cracking.

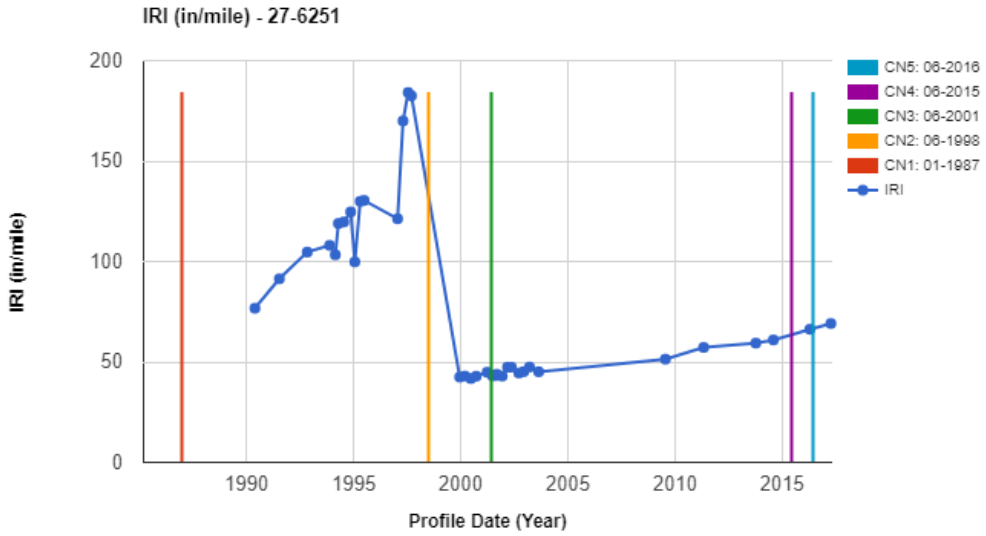

Figure 22. Time history plot of pavement roughness.

The IRI reported after the mill and overlay in 1998 does not correlate with the observed cracking during this period. Specifically, one of the predominant cracking types that purportedly affects the overall IRI of the test section—fatigue/alligator cracking—is present in higher quantities following the overlay despite the lower average IRI reported during this period. This may be related to the severity of the cracking observed on the section—predominantly low and medium prior to the 2017 manual distress survey—which plays less of a role in the roughness of the test section. Additionally, the lower amounts of transverse cracking reported after the mill and overlay, which is another cracking type that purportedly affects the overall IRI of the test section, may have played a role in the IRI observed. The transverse cracking following the mill and overlay was also predominantly low and medium severity, compared to the predominantly high severity transverse cracking reported prior to the mill and overlay.

Rutting

The average rut depths observed for the section over time are shown in Figure 23. The rutting on the section prior to the mill and overlay ranged between 0.1 and 0.3 in, but oddly enough decreased from 0.3 in (1990) to 0.1 in (1993) before increasing again to 0.2 in by 1997. Following the mill and overlay in 1998, the average rut depth dropped to slightly over 0.1 in. At that point, the average rut depth then began to increase between 2000 and 2017, with values increasing from 0.1 to 0.2 in between 2000 and 2017.

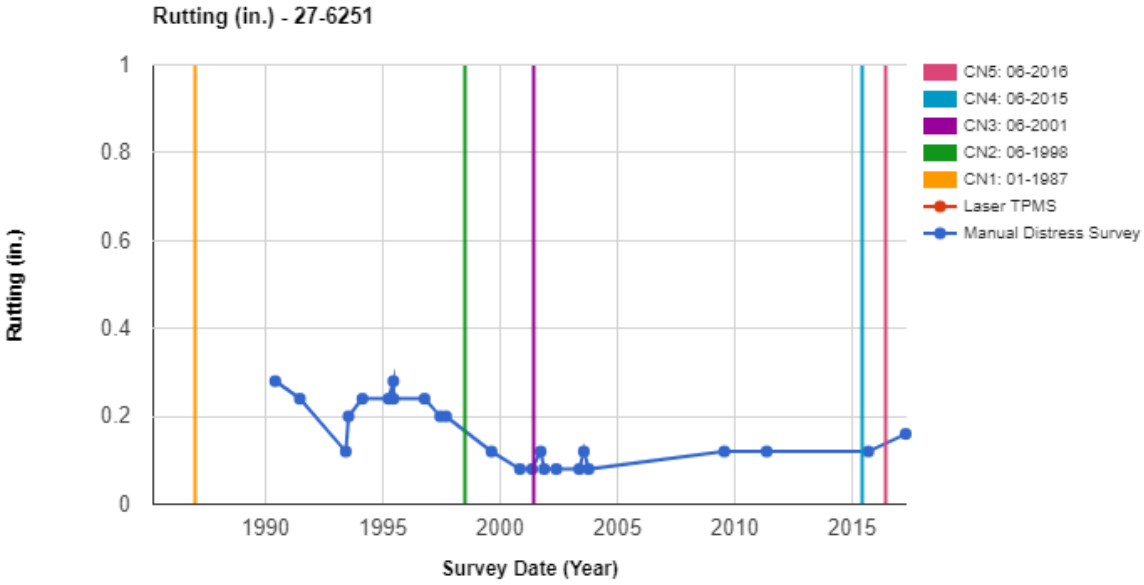

Figure 23. Time history plot of average rut depth.

In addition to the average rut depth observed over time, the change in the transverse profile of the test section was also investigated. Using the transverse profiles of the test section at multiple locations, an analysis of the predominant layer in which plastic deformation occurs was assessed using the method developed in NCHRP 01-34a.[2] The NCHRP method, which was derived using finite element analyses of rutting mechanisms in the HMA surface, base, and subgrade, is focused on the transverse profile characteristics indicative of permanent deformation such as densification, shear failure, or shear flow.

The methodology consists of two key steps: calculation of distortion parameters and the use of criteria to classify the lowest layer in the pavement structure contributing to the ruts. Distortion parameters include the maximum rut depth (D), positive area, and negative area of a transverse profile. For each profile, the wire method is used to assess the maximum rut depth, which is the greatest perpendicular distance measured from the pavement surface to the wire reference line as depicted in Figure 24. Similarly, the positive area (A_P) and negative area (A_N) are the sum of the areas above and below the transverse profile reference line, respectively. Using these parameters, the ratio of positive area to negative area (R), total area (A_T), and the theoretical total areas for the HMA, base, and subgrade failure (C_1,C_2, and C_3, respectively) are calculated and used to assess the failed layer. The assessment of the parameters used to determine the lowest layer contributing to the pavement's surface deformation is described in Figure 25.

[2] White, T., J. Haddock, A.J.T. Hand, & H. Fang. NCHRP 468: *Contributions of Pavement Structural Layers to Rutting of Hot Mix Asphalt Pavements*. National Cooperative Highway Program, Washington D.C., 2002.

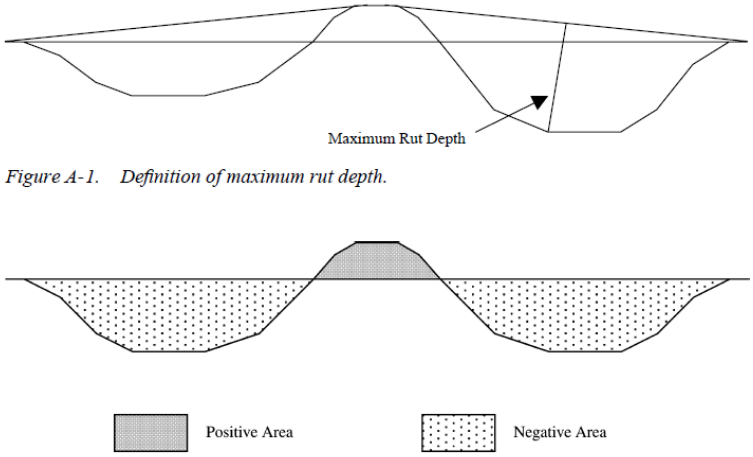

Figure A-1. Definition of maximum rut depth.

Figure 24. Transverse profile maximum rut depth and positive and negative areas (White et al., 2002)

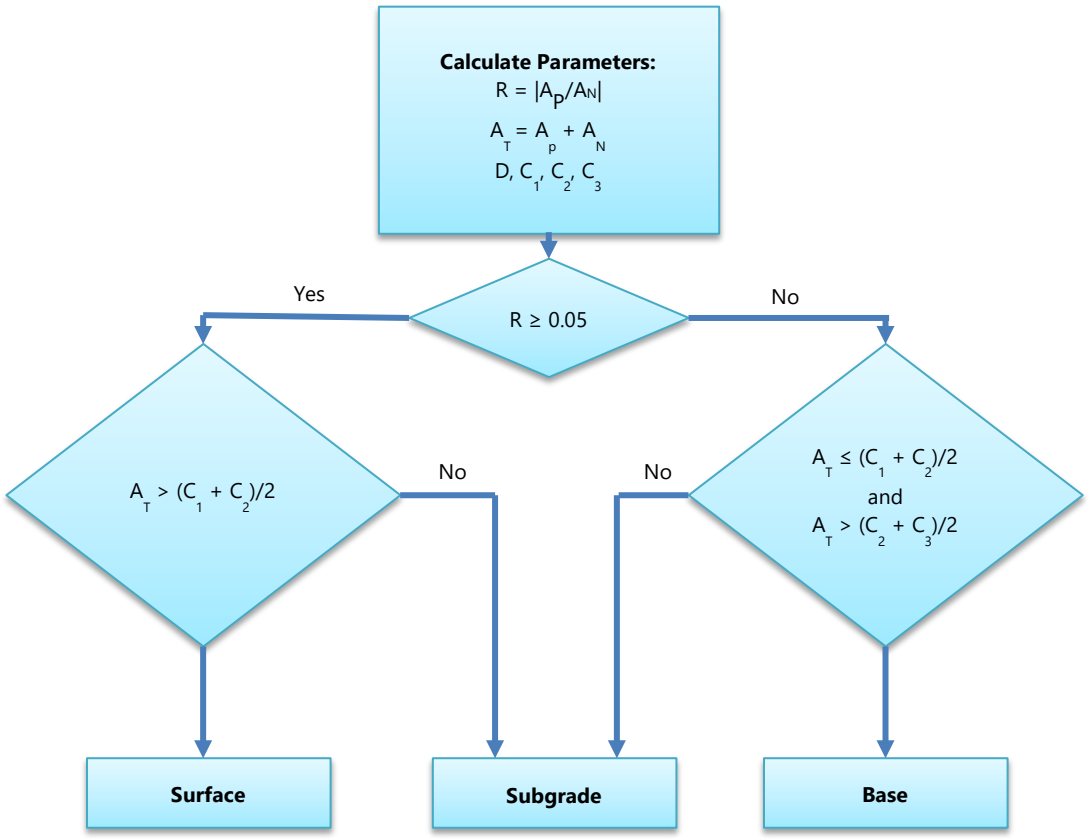

D= Maximum rut depth
A_p= Positive area (area above pavement surface line of a transverse profile)
A_n= Negative area (area below pavement surface line of a transverse profile)
C_1= (-858.21) D + 667.58, theoretical total area for HMA failure
C_2= (-1509) D -287.78, theoretical average total for base/subbase failure
C_3= (-2120.1) D – 407.95, theoretical average for subgrade failure

Figure 25. Failure layer determination using methodology by White et al. (2002)

Based on the analysis conducted for each of the transverse profiles of the test section (between 10 and 11 profiles spaced at 50 ft) for the 24 collection dates between May 1990 and April 2017, the predominant lowest layer contributing to rutting was calculated for each date of collection at multiple locations along the section. Table 6 summarizes the number of locations (or transverse profiles) along the test section where the layer most contributing to rutting was surface, base, and subgrade, respectively.

As depicted in the table, prior to the mill and overlay, the lowest contributing layer fluctuated with the base and subgrade playing a role in some locations. Following the mill and overlay, it was estimated that the surface layer played a predominant role in the rutting observed. This is likely related to the mix applied for the AC overlay, the compaction of the mix, and/or the increase in traffic over time. As the mill overlay event would have removed some of the pre-overlay rutting and resulted in a thicker overall AC layer, the unbound layers become more protected.

SUMMARY OF FINDINGS

LTPP test section 27_6251 is located on U.S. Route 2, westbound, in Beltrami County, Minnesota. U.S. Route 2 is a rural principal arterial with two lanes in the direction of traffic. The test section is classified as being in a Wet, Freeze climate zone. Test section 27_6251 constructed in January 1981 and was accepted into the LTPP Program as part of the GPS-1 experiment in January 1987. The pavement structure at the time of its incorporation into the LTPP program consisted of 7.4 inches of dense-graded asphalt concrete (AC), 10.2 inches of unbound (granular) base over a coarse-grained subgrade layer. The next construction event occurred in June 1998, when the test section received 1.6-inch mill and a 3.4-inch AC overlay, moving the section into the GPS-6S AC Overlay of Milled AC Pavement Using Conventional or Modified Asphalt study. Additional construction events that occurred on the site included crack sealing in both June 2001 and June 2015 (CN=3 and CN=4) and skin patching in June 2016 (CN=5). The test section was found to be milled and overlaid sometime after the last survey date in 2017 (the specific year of the event is still being determined), and therefore, the site has been placed OOS.

The memorandum was focused on the following:

1. **Examining the relationship between pavement deflection, pavement temperature, and subgrade moisture content.** In this study, the relationship between the average deflection, pavement temperature, and subgrade moisture content during the SMP period was assessed. To do so, a multiple linear regression analysis like the one applied for the test sections 30_8129 (Montana) and 24_1634 (Maryland) was performed. The regression coefficients for pavement temperature and moisture content were positive, which means that if either of these factors increases, the average pavement deflections will also increase. A regression model to predict deflections as a function of pavement temperature, moisture content and FWD sensor location (under the center load and 60" from the center load) was successfully developed.
2. **Identifying the cause(s) for the reduction in the reported fatigue cracking area between 2015 and 2016.** The drop in fatigue/alligator cracking in 2016 is likely due to the combination of the differences in rater opinions between the 2015 and 2017 surveys and the effects of the skin patching that occurred in 2016 (CN=5). While fatigue/alligator cracking is mostly reported in the same locations in 2015 and 2017, the rater in 2015 reported more area of low severity fatigue/alligator cracking while the 2017 rater reported smaller areas of medium and high severity fatigue/alligator cracking. Similarly, additional fatigue/alligator cracking (~13.5 ft2) was reported between stations 3+00 and 3+50 in 2015, but not in 2017. This is likely due to the difficulty in rating low severity fatigue/alligator cracking. Finally, the patching that took place in 2016 also seems to have played a role in the overall cracking reported in 2017.

Table 6. Lowest layer contributing to rutting

	Date	Number of locations where rutting was related to the surface layer	Number of locations where rutting was related to the base layer	Number of locations where rutting was related to the subgrade layer
Prior to the Mill and Overlay	05/31/1990	6	4	1
	06/18/1991	11	-	-
	06/02/1993	11	-	-
	07/14/1993	3	6	2
	02/16/1994	2	4	5
	03/30/1995	3	5	3
	06/13/1995	8	3	-
	06/15/1995	3	2	-
	10/10/1996	4	4	3
	06/11/1997	7	3	1
	09/10/1997	5	-	6
After the Mill and Overlay	08/18/1999	10	1	-
	11/02/2000	8	1	2
	05/10/2001	9	-	2
	09/21/2001	10	1	-
	11/15/2001	8	2	1
	05/23/2002	8	2	1
	05/15/2003	8	1	2
	07/26/2003	11	-	-
	10/08/2003	9	-	2
	07/21/2009	9	-	2
	05/11/2011	9	1	1
	09/10/2015	9	-	2
	04/13/2017	9	1	1

3. **Examining whether any of the non-wheel path longitudinal cracking or transverse cracking observed prior to the mill and overlay is reflected following the mill and overlay.** The NWP longitudinal cracking reported prior to the mill and overlay was predominantly located on the edge of the lane and between the wheel paths. After the overlay, the cracking was predominantly observed on the edge and centerline of the lane. Given the cracking location, it is hypothesized that the propagation of the NWP longitudinal cracking is construction-related (rather than reflection cracking) as it appears the cracking may be located along construction joints. Both prior to and following the mill and overlay event in 1998, transverse cracking was located in similar locations, indicating transverse cracking observed prior to the overlay event was reflected to the overlay surface.
4. **Identifying the potential reason(s) for the extremely low IRI on the pavement section following the overlay despite the presence of cracking throughout time.** The IRI reported on the section did not seem to be correlated to the fatigue cracking reported throughout time; while there was low IRI values reported on the test section following the mill and overlay in 1998, there was significant cracking observed. This may be related to the severity of the cracking observed on the section—predominantly low and medium—which plays less of a role in the roughness of the test section. Additionally, the lower amounts of transverse cracking reported after the mill and overlay, which is another cracking type that purportedly affects the overall IRI of the test section, may have played a role in the IRI observed. The transverse cracking following the mill and overlay was also predominantly low and medium severity, compared to the predominantly high severity transverse cracking reported prior to the mill and overlay.

FORENSIC EVALUATION RECOMMENDATIONS

While the test section was reported as active when it was initially nominated for investigation, as noted earlier, this test section was found to have been milled and overlaid following the 2017 monitoring. For this reason, no follow-up field investigations are recommended. It is suggested, however, that the FHWA LTPP Team investigate the differences between the NWP longitudinal cracking reported in the manual distress surveys and the distress information reported in InfoPave™, which are summarized in Table 7 below.

Table 7. Differences in NWP Cracking between Manual Distress Surveys and InfoPave™.

	LTPP InfoPave™ (ft)				Manual Distress Survey (ft)				
Date	L	M	H	**Total**	L	M	H	**Total**	**Total Difference (ft)**
08/24/1994	256.2	561.9	8.2	**826.3**	520.0	212.9	8.2	**741.2**	**85.1**
03/30/1995	147.9	659.3	33.8	**841.0**	222.8	567.0	43.0	**832.7**	**8.3**
08/02/1995	61.3	720.9	32.1	**814.3**	19.7	492.2		**511.8**	**302.5**
10/10/1996	112.2	634.7	66.6	**813.5**	93.5	288.4	29.2	**411.1**	**402.4**
06/11/1997	138.7	513.3	152.2	**804.2**	124.3	191.6	117.5	**433.4**	**370.8**
09/10/1997	135.1	528.1	159.7	**822.9**	121.1	176.5	121.1	**418.7**	**404.2**